SAND2020-13815C

Proceedings of the ASME 2020 Pressure Vessels & Piping Conference
PVP 2020
July 19-24, 2020, Minneapolis, MN, USA

PVP2020-21263

MEASURING FATIGUE CRACK GROWTH BEHAVIOR OF FERRITIC STEELS NEAR THRESHOLD IN HIGH PRESSURE HYDROGEN GAS

Joseph Ronevich[1], Chris San Marchi[1], Kevin A. Nibur[2], Paolo Bortot[3], Gianluca Bassanini[3], Michele Sileo[3]
[1]Sandia National Laboratories, Livermore, CA, USA
[2]Hy-Performance Materials Testing, LLC., Bend, OR, USA
[3]Tenaris-Dalmine, Dalmine, Italy

ABSTRACT

Following the ASME codes, the design of pipelines and pressure vessels for transmission or storage of high-pressure hydrogen gas requires measurements of fatigue crack growth rates at design pressure. However, performing tests in high pressure hydrogen gas can be very costly as only a few laboratories have the unique capabilities. Recently, Code Case 2938 was accepted in ASME VIII-3 allowing for master design curves to be used in lieu of performing fatigue crack growth rate (da/dN vs. ΔK) and fracture threshold (K_{IH}) testing in hydrogen gas. The master curves were based on data generated at 100 MPa H_2 on SA-372 and SA-723 grade steels; however, the data used to generate the master curves are limited to measurements of ΔK values greater than 6 MPa $m^{1/2}$. The master design curves can be extrapolated to lower ΔK (<6 MPa $m^{1/2}$), but the threshold stress intensity factor (ΔK_{th}) has not been measured in hydrogen gas. In this work, decreasing ΔK tests were performed at select hydrogen pressures to explore threshold (ΔK_{th}) for ferritic-based structural steels (e.g. pipelines and pressure vessels). The results were compared to decreasing ΔK tests in air, showing that the fatigue crack growth rates in hydrogen gas appear to overlay the curves in air at low ΔK values when tests were performed at stress ratios of 0.5 and 0.7. The results are consistent with the extrapolated master curves, which provide an upper bound throughout the entire ΔK range, even as the crack growth rates approach ΔK_{th}. This work gives further evidence to the utility of the master curves accepted into Code Case 2938 in ASME VIII-3 for construction of high pressure hydrogen vessels.

NOMENCLATURE

a	=	crack length, precrack length
a/W	=	crack length/width
ACR	=	adjusted compliance ratio
B, B_N	=	specimen thickness: actual, effective
b_o	=	remaining ligament
CT	=	compact tension
FCGR	=	fatigue crack growth rate
K	=	stress intensity factor
K_{IH}	=	fracture threshold in hydrogen
ΔK_{ACR}	=	closure corrected stress intensity factor range
ΔK_{th}	=	threshold stress intensity factor
UTS	=	ultimate tensile strength
W	=	width
YS	=	yield strength

INTRODUCTION

Hydrogen has been transmitted and stored in ferritic steel infrastructure safely for many decades, despite the fact that ferritic steels can be severely embrittled by

hydrogen. However, broad distribution of hydrogen for the transportation sector shifts the infrastructure into a different operational state that is much more exposed to pressure fluctuations. For example, a hydrogen pipeline that services a petrochemical refinery can be operated at constant pressures as the demand is constant; however, stationary storage pressure vessels at hydrogen refueling stations are subjected to fluctuations in pressure that match the demand of the consumers. The local capacity at a refueling station is not sufficient to maintain constant pressure during subsequent vehicle fills and the consequence is fatigue loading of the pressure vessels.

High pressure vessels, such as those used in hydrogen refueling stations, are designed according to the ASME Boiler and Pressure Vessel Code Section 8 Division 3, and require both fatigue crack growth rate and fracture toughness (K_{IH}) measurements in the environment. Recently, Code Case 2938 was approved which allows for use of the master design curves in lieu of performing fatigue crack growth rate and K_{IH} testing in high pressure hydrogen gas. The development of master design curves were based on the best available data generated as described previously [1], which were collected at ΔK of 6 MPa $m^{1/2}$ and higher. Since data were not collected at values below ΔK of 6 MPa $m^{1/2}$, linear extrapolation is needed and therefore an assumption is make that there is no threshold, ΔK_{th}. A ΔK_{th} most likely exists, and therefore, the master design curves are overly conservative which can limit the design life of the vessel. In addition, often times the high-pressure tanks are operated using a cascade type approach in which the tanks are operated over a narrow pressure range. Often times the tanks are refilled without dropping to their minimum pressure resulting in relatively low ΔK for that given cycle. Depending on the flaw size, operating pressure, and dimensions of the vessel, early stages of vessel life could exist in this low ΔK regime where no data have been generated to date, which presents the motivation for this current study.

Measuring fatigue crack growth rates in the low ΔK regime is quite challenging in that they require arduously long test times if performed at appropriate test frequencies. Even at 10 Hz, tests require multiple weeks to acquire sufficient data to characterize the behavior at the low da/dN range. In this paper, fatigue crack growth rates were measured in high pressure hydrogen gas in the low ΔK range ($\Delta K < 6$ MPa $m^{1/2}$) at a frequency of 10 Hz for ferritic steels. The effects of stress ratio and pressure are examined in comparison to data collected in air.

EXPERIMENTAL PROCEDURES

Materials

An SA372 Grade J material was examined which is representative of the materials commonly used in high pressure storage tanks for hydrogen refueling stations. The SA372 Gr. J material had a yield strength (YS) of 760 MPa and an ultimate tensile strength (UTS) of 890 MPa. The microstructure of the SA372 Grade J material is shown in Fig. 1a which consists of quenched and tempered martensite with carbides distributed throughout the martensite.

An API 5L X100 pipe was examined in this study and is a high strength pipeline steel grade. This material has a longitudinal YS of 732 MPa and a UTS of 868 MPa. The measured fatigue crack growth rates in hydrogen of pipeline steels with strengths ranging from YS = 352 to 700 MPa gas have exhibited negligible differences in ΔK range greater than 6 MPa $m^{1/2}$ [2]. The microstructure of the X100 steel is shown in Fig. 1b consisting of ferrite and bainite.

Two additional materials were considered in this study for comparison: 4130X (DOT-3AAX) and SA372 Grade N. Class 100 steel. We did not obtain micrographs of their microstructure. However, broadly speaking, the microstructure of both materials consist of quenched and tempered martensite. The 4130X has a yield strength of 641 MPa and UTS of 786 MPa. The minimum requirements for SA372 Grade N Cl. 100 are YS > 690 MPa and UTS between 795 and 965 MPa. The compositions for X100, SA372 Grade J, and 4130X can be found in Table 1.

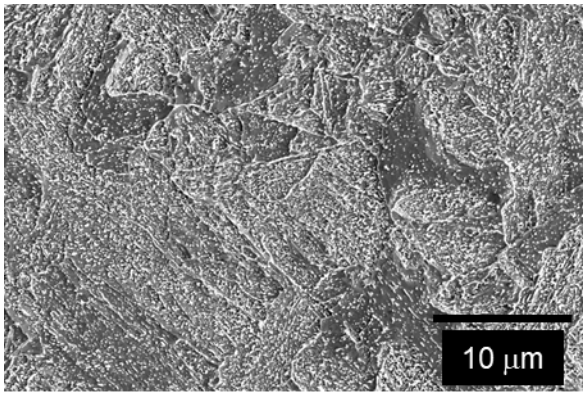

(a)

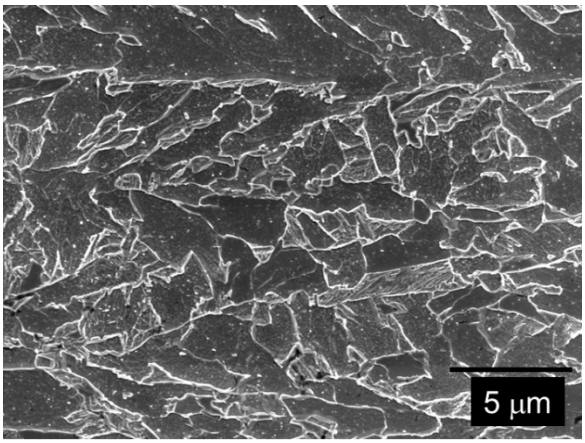

(b)

Figure 1 – Scanning electron microscope images of (a) SA372 Grade J, (b) X100 pipeline steel. Etched 2% nital.

Specimen Preparation

Compact tension (CT) specimens were extracted from the steel vessels and pipes such that the load would be applied in the orientation consistent with the hoop direction and the crack would advance in the axial direction. Specimens were machined according to ASTM E647 [3] with a width (W) of 26.4 mm, thickness (B) of 12.7 mm, a notch length to width ratio of 0.2. Additionally side grooves were machined to reduce thickness (B_N) of 11.2 mm. Specimens were precracked in two stages: compression-compression precracking to initiate a crack followed by tension-tension precracking to advance the crack [4]. The compression-compression precracking was accomplished through rigid test fixtures and pin loading in compression to minimum loads of -13.3 kN (-3,000 lbf) at a stress ratio R=0.05. This procedure typically initiated and advanced the crack approximately 0.2 mm. Subsequent tension-tension precracking was used to extend the crack an additional 3-5 mm at K_{max} values of 11 MPa $m^{1/2}$ at R=0.1 to final crack lengths to width ratios (a/W) of approximately 0.34 to 0.38.

Fatigue Crack Growth Rate Measurements

Tests were executed under K-control under decreasing K-gradient (e.g. K-shed), where K is the stress intensity factor. As the goal of this work was to measure the low ΔK-regime, a frequency of 10 Hz was used to make test duration manageable. In addition, the K-gradient [3] was controlled at either -0.31 or -0.39 mm^{-1} to help reduce test time. Despite these efforts to reduce test duration, each FCGR curve at each stress ratio required over 1 week to complete. Tests were completed at stress ratios of 0.5 and 0.7 as these are applicable to how high pressure storage tanks are operated at hydrogen refueling stations.

Fatigue crack growth rate testing was performed in air and high purity (99.9999%) high pressure hydrogen gas. Samples were placed in our custom-build pressure vessel which is located in a servo-hydraulic load frame. The high pressure testing system is equipped with dynamic seals to allow for concurrent loading while under pressure. For more details on the specifics in the testing capabilities, please see [5]. Tests were performed at 293 K and at pressures of either 21 or 100 MPa H_2. Maintaining a good seal is critical to accomplishing long-term tests and higher pressures combined with high frequencies generate significant wear on the seals resulting in shorter seal lifetimes. The consequence is that only a single test was completed at 100 MPa H_2 as long durations were not deemed to be feasible. The compromise was to perform the remainder of the tests at 21 MPa which allowed for lower pressure seals that perform better under these conditions.

Prior to starting any test in high pressure hydrogen gas, the system was leak checked at test pressure with helium, followed by four successive purges with nitrogen to 14 MPa, and four successive purges with hydrogen to 14 MPa. The system was then filled to the test pressure and the transducers were allowed to equilibrate (typically 48 hr) before starting the test. A strain-based clip gauge was used to measure load-line displacement and an internal load cell was used to measure load directly applied to the sample. Load, crack length, and crack opening displacement were recorded every 0.05 mm.

The crack growth rate (da/dN) as a function of stress intensity factor (ΔK) was calculated following a seven point polynomial method outlined in ASTM E647 [3]. At the completion of the tests, the samples were fatigued open in air to allow inspection of the fracture surfaces. Optical measurements were used to correct the unloading compliance calculated crack lengths. The ΔK was corrected for crack closure via the adjusted compliance ratio (ACR) method described in [6] and applied through the Fracture Technology Associates (FTA) software. The subsequent plots of FCGR were plotted as da/dN vs ΔK_{ACR} to acknowledge that the data were corrected for crack closure, if closure occurred.

Figure 2 shows an optical image of an X100 specimen after fracturing open. Within the precrack region, a small crack can be observed which extended during the compression-compression precracking. This was followed by the tension-tension precracking. The crack extensions in 21 MPa H_2 are clearly observable at the two stress ratios of R=0.5 and R=0.7. A rising-displacement fracture test was completed in 21 MPa H_2 following the fatigue which shows the extremely rough surface. The results of the fracture toughness tests are not discussed further in this

paper. Overall, uniform crack fronts were observed in the materials tested as shown in Fig. 2, below.

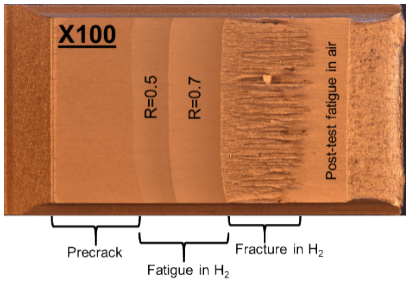

Figure 2 – Optical image of fractured X100 specimen. There are several distinct regions observable on the fracture surface: precrack in air, K-shed at R=0.5 in H_2, K-shed at R=0.7 in H_2, fracture test in H_2, followed by post-fatigue in air to separate the specimen.

RESULTS

Fatigue crack growth rate tests at low ΔK

Fatigue crack growth rates were measured in both air and high pressure hydrogen gas at stress ratios of R=0.5 and R=0.7. The focus was to measure da/dN at lower ΔK ranges; however, as da/dN decreases the test duration can become exceedingly long and therefore test frequencies of 10 Hz were utilized. Figure 3 shows the FCGR curves of X100 steel tested in both air and 21 MPa H_2. Tests in hydrogen at higher ΔK were performed at 1 Hz compared to tests at lower ΔK, which were performed at 10 Hz. At ΔK values greater than 8 MPa $m^{1/2}$, a clear acceleration can be observed of FCGR in hydrogen compared to in air. At ΔK less than 6 MPa $m^{1/2}$, the curves exhibit significant overlap and it appears that the curves in hydrogen fall below the curves in air. The influence of stress ratio (R) is observed in the curves, meaning that the higher stress ratio results in higher FCGR for a given ΔK [7]. This trend is observed across the entire ΔK range tested. Also shown in Fig. 3 are two master curves taken from the ASME BPVC Code Case 2938. These represent design master curves that have been approved for use with SA-372 and SA-723 steels for ASME Section VIII, Div 3 construction. Although these curves are currently limited to use for SA-372 and SA-723, we have used these curves as a way to demonstrate their utility among a variety of ferritic steels that will be presented in Figures 3-6. The design master curves accommodate stress ratio and therefore there are two for these figures: R=0.5 and R=0.7.

Despite the high stress ratios of 0.5 and 0.7, low ΔK tests are still susceptible to crack closure. To account for potential crack closure, the adjusted compliance ratio (ACR) was used to remove crack closure effects. Figure 4 shows the crack growth rates (da/dN) versus the closure corrected stress intensity factor range (ΔK_{ACR}). The curves tested at stress ratios of 0.5 are more likely to exhibit crack closure than tests at R=0.7. This becomes obvious as you compare the FCGR curves in Fig. 3 and Fig. 4 as the FCGR curves for R=0.5 shift when corrected for closure. The higher stress ratio tests at R=0.7 exhibit a negligible shift as closure is less likely to occur. After corrected for closure, the X100 FCGR curves (Fig. 4) at low ΔK appear to overlap better between the air and H_2 experiments. The subsequent plots for SA372 Grade J and 4130X show only the ΔK_{ACR} comparison once closure is accounted for. Similar shifts were observed, with the R=0.5 showing more shift than the R=0.7.

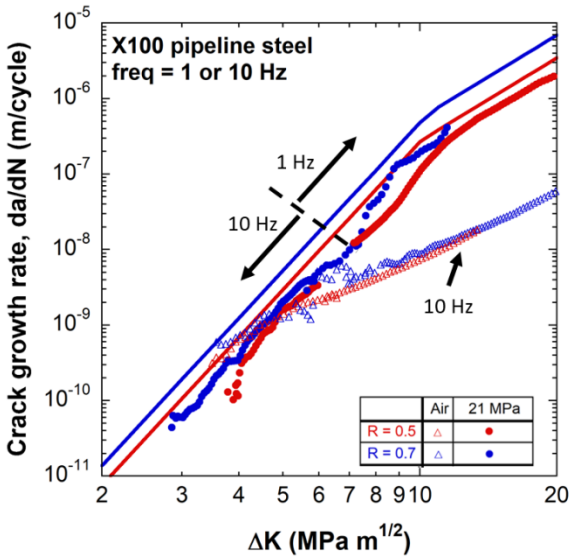

Figure 3 – Fatigue crack growth rate (da/dN vs ΔK) curves of X100 pipeline steel tested in air and 21 MPa H_2.

ASTM E647 [3] discusses an operational ΔK_{th} as being the FCGR at 10^{-10} m/cycle. Although it does not appear that a true ΔK_{th} is attained in our data sets, the operational ΔK_{th} for the tests performed in hydrogen appear to fall between 3 and 4 MPa $m^{1/2}$. The operational ΔK_{th} is observed to be lower for the higher stress ratio of R=0.7 as expected. For subsequent discussion, the operational ΔK_{th} will be discussed as just the ΔK_{th}.

Figure 5 shows the FCGR curves for SA372 Grade J tested in air, 21 MPa H_2, and 105 MPa H_2. Tests were conducted at 10 Hz and at stress ratios of R=0.5 and R=0.7. For comparsion, SA372 Grade N Class 100 data are shown in air tested at R=0.7. Both SA372 Grade J and Grade N show very similar behavior in air at R=0.7. The single test performed in 105 MPa H_2 at R=0.5 exhibits a higher FCGR

than the 21 MPa H_2 test in the low ΔK range (e.g. 4-5 MPa $m^{1/2}$). It is commonly observed that higher pressures result in higher FCGR at lower ΔK range (e.g. >6 MPa $m^{1/2}$) [8] which then levels out at higher ΔK. Similar to the X100 steel, the FCGR curves in air and H_2 appear to converge near ΔK_{th}. The ΔK_{th} values were measured to be similar to the X100 with values between 3-4 MPa $m^{1/2}$. The design master curves capture the FCGR behavior very well over the entire ΔK range in Fig. 5.

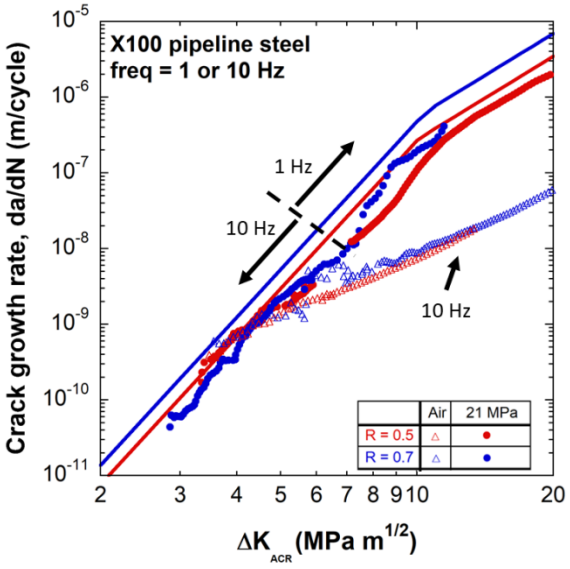

Figure 4 – Fatigue crack growth rate curves (da/dN vs. ΔK_{ACR}) of X100 pipeline steel tested in air and 21 MPa H_2. The tests at R=0.5 exhibit greater shifts than R=0.7 if compared to Fig. 3.

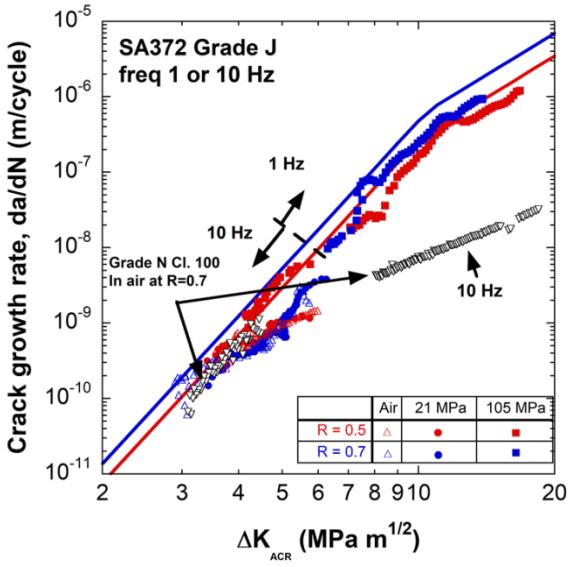

Figure 5 – Fatigue crack growth rate (da/dN vs. ΔK_{ACR}) curves of SA372 Grade J pressure vessel steel tested in air and 21 MPa H_2 and 105 MPa H_2. Also shown are SA372 Grade N Cl. 100 tested at R=0.7 in air.

Figure 6 shows FCGR curves of the 4130X, also designated as DOT-3AAX, which are conventionally used for fabrication of laboratory gas cylinders. FCGR tests were performed in air and 21 MPa at stress ratios of R=0.5 and R=0.7 at a frequency of 10 Hz. The FCGRs appear to overlay in air and H_2 in the ΔK range from 5-6 MPa $m^{1/2}$. In the 4130X, the FCGR values in 21 MPa H_2 appear to fall below the air data. This is slightly different than observed in the SA372 Grade J. The X100 exhibits a slightly lower FCGR in 21 MPa H_2 but it is difficult to consider that a trend with this limited data set. The FCGR curves in air appear to exhibit more of a visible ΔK_{th} (meaning the curve turns down) than in H_2, however the values attain 10^{-10} m/cycle between 3 and 4 MPa $m^{1/2}$. The design master curves provide a clear upper bound to the 4130X steels tested in 21 MPa H_2.

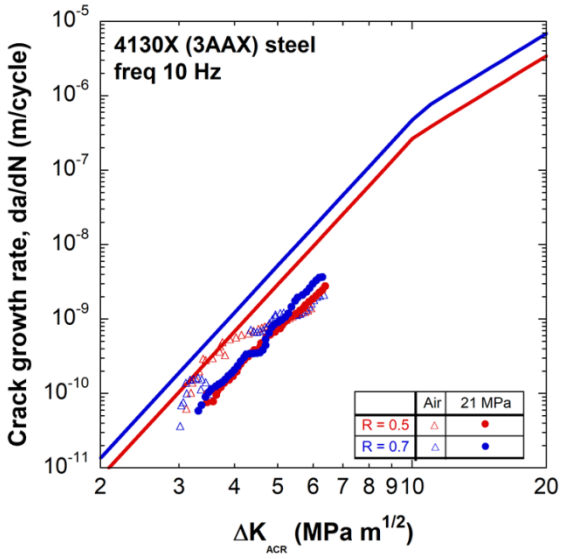

Figure 6 – Fatigue crack growth rate (da/dN vs. ΔK_{ACR}) curves of 4130X steel tested in air and 21 MPa H_2.

Fracture surfaces of fatigue samples

Select samples of the X100 pipeline specimens were examined in a scanning electron microscope to observe features on the fracture surfaces. The results are shown in Fig. 7 for X100 tested in 21 MPa H_2 at a stress ratio of R=0.5. The crack front in all the fracture surface images extends from bottom to top of the images. Figure 7a shows the fracture surface near in the low ΔK range (e.g. ~3.8 MPa $m^{1/2}$) which features fatigue striations commonly observed in ferritic steels tested in an air environment. An

enlarged image is shown in Fig. 7a with white arrows pointing to the rough striations. Figure 8 shows these fatigue striations very clearly on the fracture surface of an X52 pipeline steel tested in air at $\Delta K \sim 8$ MPa $m^{1/2}$ and is representative of the typical features on ferritic steel fracture surfaces when tested in air. The white arrows in both Fig. 7a and Fig. 8 point to perturbations on fracture surfaces that appear to be striations that suggest a blunting and resharpening during crack growth.

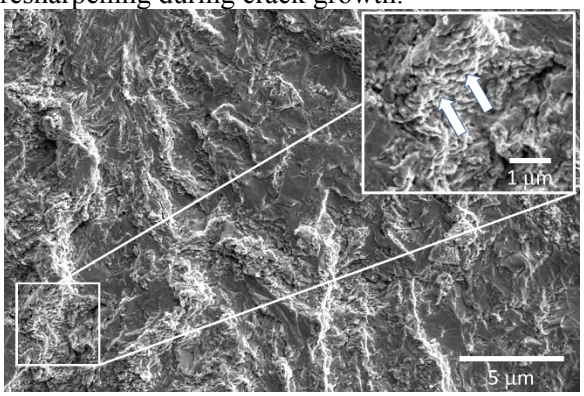

(a)

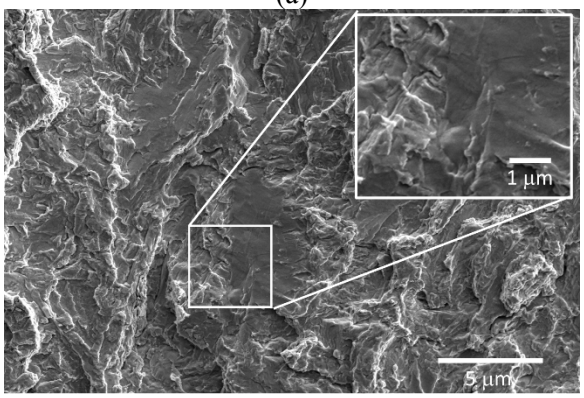

(b)

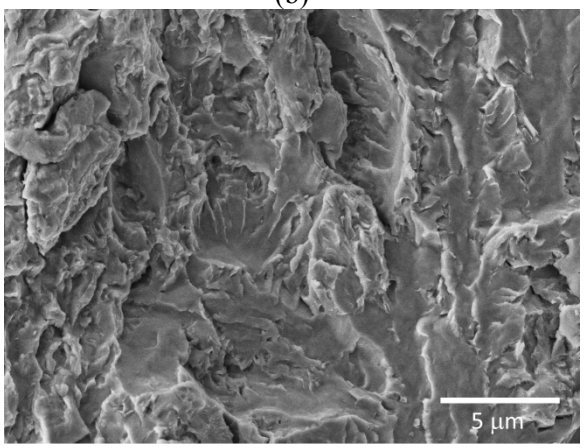

(c)

Figure 7 – Scanning electron microscope images of X100 fracture surfaces for FCGR tests performed in 21 MPa H_2 at stress ratio R=0.5: (a) $\Delta K \sim 3.8$ MPa $m^{1/2}$, (b) $\Delta K \sim 6$ MPa $m^{1/2}$, (c) $\Delta K > 15$ MPa $m^{1/2}$. The arrows in (a) point to fatigue striations.

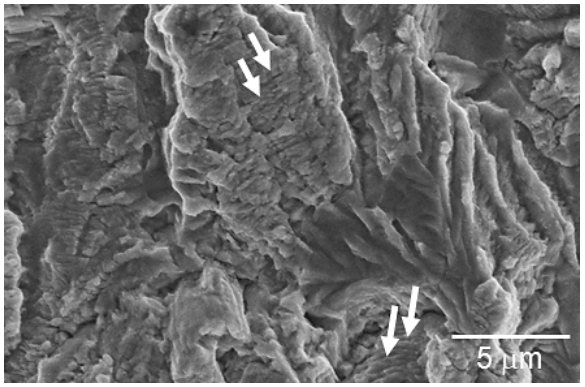

Figure 8 – Scanning electron microscope image of X52 pipeline steel fatigue tested in air a $\Delta K \sim 8$ MPa $m^{1/2}$. Arrows point to fatigue striations.

Figure 7b shows the fracture surface of X100 pipeline steel tested in 21 MPa H_2 at a $\Delta K \sim 6$ MPa $m^{1/2}$. The characteristic features on the fracture surface are larger flat regions with less roughness overall. The enlarged region shows that there is a noticeable absence of striations. Figure 7c shows the X100 pipeline steel at higher $\Delta K > 15$ MPa $m^{1/2}$ in 21 MPa H_2. The features in Fig. 7c are comparable to the Fig. 7b in which there is a notable absence of striations on the surface.

DISCUSSION

Three different ferritic steels were tested in the low ΔK range in high pressure hydrogen gas at stress ratios R=0.5 and R=0.7. The results showed remarkably similar behavior of all the steels in this ΔK range. Although a truly visible ΔK_{th} was not apparent (e.g. indicated by the da/dN becoming asymptotic), data were generated down to 10^{-10} m/cycle, which for engineering purposes has been deemed an operational threshold [3]. The ΔK_{th} measured for the ferritic steels ranged between 3 and 4 $MPa^{1/2}$. It is clear that the FCGR data in air and hydrogen appear to begin to overlap around a $\Delta K \sim 5$ MPa $m^{1/2}$. Previous data generated at only higher ΔK often speculated that the curves would converge at lower ΔK [9-11] but this work provides clear evidence that the curves do converge. When corrected for closure, the X100 (Fig. 4) and SA372 Grade J (Fig. 5) show consistent FCGR between air and hydrogen environments. The 4130X steel is unique in that the 21 MPa H_2 curves fall below the air curves for both R=0.5 and R=0.7. The reason for this is not clear. The convergence of the curves, similar to the X100 and SA372 Grade J, has been observed previously [7], albeit at low pressures. The principle [7]

behind this is that at low ΔK, the effects of hydrogen are diminished and hydrogen is effectively acting as inert gas, providing an oxygen and moisture free environment. In previous work [7], the FCGR curves near ΔK_{th} were observed to converge between tests in air and H_2 when high stress ratios were implemented. At lower stress ratios, air tests resulted in higher ΔK_{th} due to oxide-induced closure [7]. Therefore, it is still unclear as to why the FCGRs of the 4130X tested in H_2 fall below the air curves as any effect of moisture or oxygen should result in the air curves exhibiting a higher ΔK_{th}. More testing may clarify if this is a repeatable trend.

The striations observed in Fig. 7a indicate a blunting and resharpening mechanism is occurring, which is commonly observed on fracture surfaces in air (Fig. 8). This is not conventionally observed in tests in H_2 on ferritic steels [10, 11] when tested at higher ΔK. Striations observed on the fracture surface near ΔK_{th} in H_2 suggests that the effects of hydrogen are diminished. Hydrogen is typically associated with requiring less plasticity to extend a crack and therefore the crack remains sharper during fatigue. This is likely why we do not observe the striations at higher ΔK values where crack growth rates are high. However, when the ΔK is low enough, the effects of hydrogen are diminished and conventional fatigue occurs via a blunting and resharpening mechanism. This is complemented by the convergance of FCGR between the H_2 and air data.

The test frequency for the ΔK_{th} experiments was 10 Hz due to necessity to complete the tests in a reasonable amount of time. Tests in hydrogen gas as a function of frequency have been examined at higher ΔK ranges [9] which showed less than a factor of 2-3 lower FCGR at 10 Hz compared to 1 Hz. At lower frequencies, the difference completely diminished. Lower frequencies have not been tested near the ΔK_{th} range and it may not be realistic to perform these tests; however, the extrapolation of the data generated at 1 Hz at higher ΔK seems comparable to the data generated at 10 Hz at lower ΔK. This suggests that test frequency may play less of a role at lower ΔK, where FCGRs are greatly reduced.

The design master curves from ASME Code Case 2938 for R=0.5 and R=0.7 provide an upper bound curve for all the data generated in this paper over a wide range of hydrogen pressures. If the master curves are used for design, they appear to provide a conservative estimate of the FCGR down to an operational ΔK_{th} of 10^{-10} m/cycle. This observation provides further testament to the utility of the design master curves as the linear trend of the master curves appear consistent with the data generated down to 10^{-10} m/cycle. The ΔK experienced by a pressure vessel or pipeline in service is dependent on many factors including design, operation, flaw size, and use of autofrettage. While one could argue that a crack growing at 10^{-10} m/cycle is not significant, the reality is that pressure vessels and pipes may be operating at low ΔK for a large portion of their lives. Generating data in hydrogen near ΔK_{th} could help influence how we determine design criteria for these vessels in the future, particularly if a true ΔK_{th} can be established. The fact that the FCGRs in hydrogen appear to become coincident or below those in air could perhaps influence future designs and reduce overly conservative margins.

SUMMARY

Fatigue crack growth rates on ferritic steels were measured at low ΔK in high pressure hydrogen gas and air at stress ratios of R=0.5 and R=0.7. Despite these high stress ratios, crack closure was observed at the low ΔK particularly at R=0.5. The adjusted compliance ratio (ACR) correction was applied to removed the effects of crack closure. FCGR curves (da/dN vs. ΔK_{ACR}) in air and hydrogen showed convergence in the low ΔK range. Operational ΔK_{th} (e.g. da/dN ~ 10^{-10} m/cycle) were measured to be between 3 and 4 MPa $m^{1/2}$ and exhibited remarkable consistency between the pressure vessel steels (SA372 and 4130X) and pipeline steel (X100) tested. Design master curves from ASME Code Case 2938 provided an upper bound for the data and captured the behavior down to ΔK_{th} demonstrating the utility of the master curves over a broad range of ΔK. Near ΔK_{th}, the fracture surfaces exhibited fatigue striations which are commonly observed in tests in air, but are typically absent in hydrogen environments where crack growth rates are accelerated. The effect of hydrogen appears to be dimished in the low ΔK range indicated by the convergance of FCGR and similar fracture appearance to the tests performed in air.

ACKNOWLEDGMENTS

The authors are grateful to B. Davis and J. McNair for support of high pressure testing, A. Gardea, H.Vega for metallographic preparation, and W. York and R. Nishimoto for SEM imaging. Sandia National Laboratories is a multimission laboratory managed and operated by National Technology and Engineering Solutions of Sandia, LLC., a wholly owned subsidiary of Honeywell International, Inc., for the U.S. Department of Energy's

National Nuclear Security Administration under contract DE-NA-0003525.

Table 1 – Chemical Compositions for Steels (in wt%)

	Cr	Mo	Mn	Si	C	Fe
X100	0.19	0.17	1.69	0.26	0.085	Bal
SA372 Gr. J	0.99	0.18	0.93	0.28	0.49	Bal
4130X	0.95	0.18	0.63	0.28	0.30	Bal

REFERENCES

[1] C. San Marchi, J. Ronevich, P. Bortot, Y. Wada, J. Felbaum, and M. Rana, "Technical basis for master curve for fatigue crack growth of ferritic steels in high-pressure gaseous hydrogen in ASME Section VIII-3 code PVP2019-93907," presented at the Proceedings of the ASME 2019 Pressure Vessels & Piping Conference, San Antonio, TX, July 14-19, 2019.

[2] J. Ronevich and B. Somerday, "Hydrogen-Accelerated Fatigue Crack Growth in Arc Welded X100 Pipeline Steel," in *Materials Performance in Hydrogen Environments: Proceedings of the 2016 International Hydrogen Conference*, Jackson Hole, WY, B. P. Somerday and P. Sofronis, Eds., 2016: ASME, pp. 219-227.

[3] *E647-11 Standard Test Method for Measurement of Fatigue Crack Growth Rates*, ASTM, West Conshohocken, PA, 2011.

[4] J. C. Newman and Y. Yamada, "Compression precracking methods to generate near-threshold fatigue-crack-growth-rate data," *International Journal of Fatigue,* vol. 32, no. 6, pp. 879-885, 2010/06/01/ 2010, doi: https://doi.org/10.1016/j.ijfatigue.2009.02.030.

[5] B. P. Somerday, J. A. Campbell, K. L. Lee, J. A. Ronevich, and C. San Marchi, "Enhancing safety of hydrogen containment components through materials testing under in-service conditions," *International Journal of Hydrogen Energy,* vol. 42, pp. 7314-7321, 2017, doi: 10.1016/j.ijhydene.2016.04.189.

[6] J. K. Donald, "Introducing the compliance ratio concept for determining effective stress intensity," *International Journal of Fatigue,* vol. 19, no. 93, pp. 191-195, 1997, doi: http://dx.doi.org/10.1016/S0142-1123(97)00024-8.

[7] S. Suresh and R. O. Ritchie, "Mechanisitic dissimilarities between environmentally influenced fatigue-crack propagation at near-threshold and higher growth rates in lower strength steels," *Metal Science,* vol. 16, pp. 529-538, 1982.

[8] C. San Marchi, B. P. Somerday, K. A. Nibur, D. G. Stalheim, T. Boggess, and S. Jansto, "Fracture and Fatigue of Commercial Grade API Pipeline Steels in Gaseous Hydrogen," presented at the ASME 2010 Pressure Vessels & Piping Division, Bellevue, Washington USA, 2010.

[9] B. Somerday, P. Bortot, and J. Felbaum, "Optimizing measurement of fatigue crack growth relationships for Cr-Mo pressure vessel steels in hydrogen gas," presented at the ASME 2015 Pressure Vessels and Piping Conference, Boston, MA, July 19-23, 2015, 2015.

[10] B. P. Somerday, P. Sofronis, K. A. Nibur, C. San Marchi, and R. Kirchheim, "Elucidating the variables affecting accelerated fatigue crack growth of steels in hydrogen gas with low oxygen concentrations," *Acta Materialia,* vol. 61, no. 16, pp. 6153-6170, 2013, doi: http://dx.doi.org/10.1016/j.actamat.2013.07.001.

[11] J. A. Ronevich, B. P. Somerday, and C. San Marchi, "Effects of microstructure banding on hydrogen assisted fatigue crack growth in X65 pipeline steels," *International Journal of Fatigue,* vol. 82, no. Part 3, pp. 497-504, 2016/01/01/ 2016, doi: https://doi.org/10.1016/j.ijfatigue.2015.09.004.